

13. Bauer, G. E. W., Tserkovnyak, Y., Huertas-Hernando, D. & Brataas, A. Universal angular magnetoresistance and spin torque in ferromagnetic/normal metal hybrids. *Phys. Rev. B* **67**, 094421 (2003).
14. Rippard, W. H., Pufall, M. R. & Silva, T. J. Quantitative studies of spin-momentum-transfer-induced excitations in Co/Cu multilayer films using point-contact spectroscopy. *Appl. Phys. Lett.* **82**, 1260–1262 (2003).
15. Özyilmaz, B. *et al.* Current-induced magnetization reversal in high magnetic fields in Co/Cu/Co nanopillars. *Phys. Rev. Lett.* **91**, 067203 (2003).
16. Urazhdin, S., Birge, N. O., Pratt, W. P. Jr & Bass, J. Current-driven magnetic excitations in permalloy-based multilayer nanopillars. Preprint at (<http://arXiv:cond-mat/0303149>) (2003).
17. Albert, F. J. *The Fabrication and Measurement of Current Perpendicular to the Plane Magnetic Nanostructures for the Study of the Spin Transfer Effect*. PhD dissertation, Cornell Univ. (2003).
18. Baibich, M. N. *et al.* Giant magnetoresistance of (001)Fe/(001)Cr magnetic superlattices. *Phys. Rev. Lett.* **61**, 2472–2475 (1988).
19. Pozar, D. M. *Microwave Engineering* 2nd edn, 566 (John Wiley & Sons, New York, 1998).
20. Kittel, C. *Introduction to Solid State Physics* 7th edn, 505 (John Wiley & Sons, New York, 1996).
21. Johnson, M. T., Bloemen, P. J. H., den Broeder, F. J. A. & de Vries, J. J. Magnetic anisotropy in metallic multilayers. *Rep. Prog. Phys.* **59**, 1409–1458 (1996).
22. Lee, C. H. *et al.* Magnetic anisotropy in epitaxial Co superlattices. *Phys. Rev. B* **42**, 1066–1069 (1990).
23. Myers, E. B. *et al.* Thermally activated magnetic reversal induced by a spin-polarized current. *Phys. Rev. Lett.* **89**, 196801 (2002).
24. Nazarov, A. V., Cho, H. S., Nowak, J., Stokes, S. & Tabat, N. Tunable ferromagnetic resonance peak in tunneling magnetoresistive sensor structures. *Appl. Phys. Lett.* **81**, 4559–4561 (2002).
25. Sun, J. Z. Spin-current interaction with a monodomain magnetic body: A model study. *Phys. Rev. B* **62**, 570–578 (2000).
26. Bazaliy, Y. B., Jones, B. A. & Zhang, S. C. Towards metallic magnetic memory: How to interpret experimental results on magnetic switching induced by spin-polarized currents. *J. Appl. Phys.* **89**, 6793–6795 (2001).
27. Grolier, J. *et al.* Field dependence of magnetization reversal by spin transfer. *Phys. Rev. B* **67**, 174402 (2003).
28. Li, Z. & Zhang, S. Magnetization dynamics with a spin-transfer torque. *Phys. Rev. B* **68**, 024404 (2003).
29. Suhl, H. The theory of ferromagnetic resonance at high signal powers. *J. Phys. Chem. Solids* **1**, 209–227 (1957).
30. Polianski, M. & Brouwer, P. W. Current-induced transverse spin wave instability in a thin nanomagnet. Preprint at (<http://arXiv:cond-mat/0304069>) (2003).

Acknowledgements We thank K. W. Lehnert, I. Siddiqi and other members of the groups of R. J. Schoelkopf, D. E. Prober and M. H. Devoret for advice about microwave measurements. We acknowledge support from DARPA through Motorola, from the Army Research Office, and from the NSF/NSEC programme through the Cornell Center for Nanoscale Systems. We also acknowledge use of the NSF-supported Cornell Nanofabrication Facility/NNUN.

Competing interests statement The authors declare that they have no competing financial interests.

Correspondence and requests for materials should be addressed to D.C.R. (ralph@ccmr.cornell.edu).

Video-speed electronic paper based on electrowetting

Robert A. Hayes & B. J. Feenstra

Philips Research Eindhoven, Prof. Holstlaan 4, 5656 AA Eindhoven, The Netherlands

In recent years, a number of different technologies have been proposed for use in reflective displays^{1–3}. One of the most appealing applications of a reflective display is electronic paper, which combines the desirable viewing characteristics of conventional printed paper with the ability to manipulate the displayed information electronically. Electronic paper based on the electrophoretic motion of particles inside small capsules has been demonstrated¹ and commercialized; but the response speed of such a system is rather slow, limited by the velocity of the particles. Recently, we have demonstrated that electrowetting is an attractive technology for the rapid manipulation of liquids on a micrometre scale⁴. Here we show that electrowetting can also be used to form the basis of a reflective display that is significantly faster than electrophoretic displays, so that video content can be displayed. Our display principle utilizes the voltage-controlled movement of a coloured oil film adjacent to a white substrate.

The reflectivity and contrast of our system approach those of paper. In addition, we demonstrate a colour concept, which is intrinsically four times brighter than reflective liquid-crystal displays⁵ and twice as bright as other emerging technologies^{1–3}. The principle of microfluidic motion at low voltages is applicable in a wide range of electro-optic devices.

Microfluidic movement based on electrowetting^{4,6,7}—where a voltage difference between a hydrophobic solid and a liquid causes a change in wettability—is being used for an increasing number of applications. These include pixelated optical filters⁴, adaptive lenses⁸ and lab-on-a-chip⁹. Electrowetting has several very attractive features for use in micrometre- to millimetre-sized systems: low power consumption, fast response speed and scalability. In addition, when a fluoropolymer coating with low contact-angle hysteresis is used, a high degree of reversibility can be obtained⁴. However, in most of the applications reported a thick insulator is used, giving rise to high switching voltages. By improving the processing of hydrophobic insulating materials we managed to lower the drive voltages dramatically^{10,11}, opening up a much broader application area.

For the electrowetting display principle, the focus is on the movement of a confined water–oil interface (Fig. 1). In equilibrium, a coloured oil film lies naturally between the water and the hydrophobic insulator coating of an electrode, because

$$\gamma_{o,w} + \gamma_{o,i} < \gamma_{w,i} \quad (1)$$

where γ is the interfacial tension, and the subscripts denote the oil, water and insulator, respectively. Owing to the dominance of interfacial over gravitational forces in small systems (<2 mm), such an oil film is continuous and stable in all orientations. However, when a voltage V is applied between the substrate electrode and the water, an electrostatic term ($\sim 0.5CV^2$, where C is the parallel-plate capacitance) is added to the energy balance, and the stacked state is no longer energetically favourable (Fig. 1b). The system can lower its energy by moving the water into contact with the insulator, thereby displacing the oil.

The balance between electrical and capillary forces determines how far the oil is moved to the side. Hence the optical properties of the stack, when viewed from above, can be continuously and reversibly tuned between a coloured off-state and a transparent on-state, assuming that the pixel is sufficiently small that a viewer

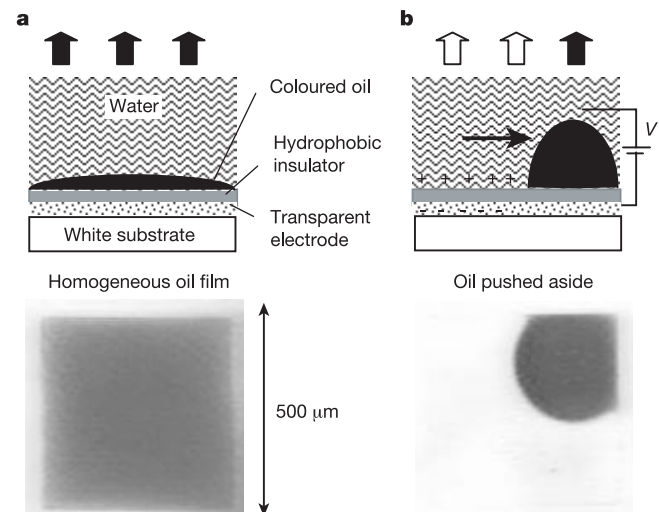


Figure 1 Electrowetting display principle. **a**, No voltage applied, therefore a coloured homogeneous oil film is present. **b**, d.c. voltage applied, causing the oil film to contract. Top row, diagrams; bottom row, photographs. The photographs show typical oil motion obtained with an homogeneous pixel electrode.

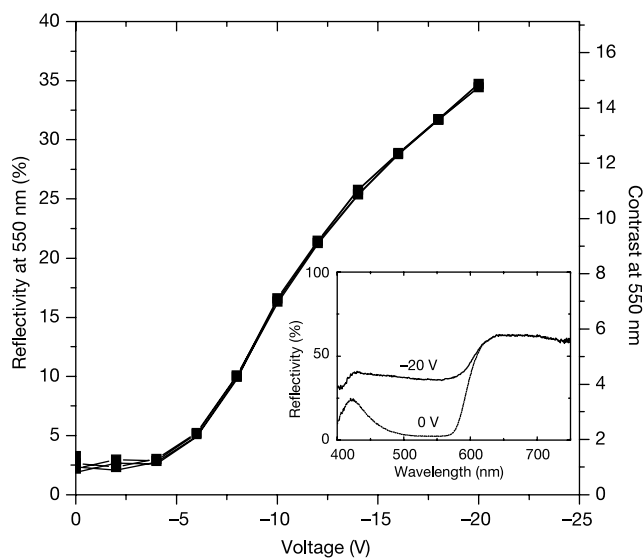


Figure 2 Electro-optic behaviour of electrowetting display pixels. Reflectivity and contrast as a function of d.c. voltage for a $500 \times 500 \mu\text{m}^2$ pixel with a $15\text{-}\mu\text{m}$ -thick magenta oil layer and a $0.8\text{-}\mu\text{m}$ -thick fluoropolymer insulator. Inset, full wavelength response.

experiences the average optical response. Alternatively, if a diffusely reflective (white) surface is placed under the switchable element, a simple high-brightness/high-contrast optical switch is obtained that can be used as the basis for a reflective display. It has been previously proposed¹² that electrowetting could be used as a display principle by driving a refractive index matched liquid into a three-dimensional porous network to provide the optical modulation from white to transparent. Optical performance aside, applying the metallic and insulating layers required for reversible electrowetting in such a porous network renders this principle highly impractical. In contrast, the microfluidic motion demonstrated here is two-dimensional, which can be practically realized using the currently available (and reliable) electrowetting device materials over large display areas.

In our system, the white reflector is integrated into the optical stack by coating a white polymer foil with a thin, patterned (15 nm indium tin oxide, ITO) electrode layer and a fluoropolymer insulator. The moving oil film is now separated from the white substrate by just the thickness of the electrode/insulator combination (typically $<1\ \mu\text{m}$), resulting in a very efficient recycling of ambient light. Oils of any required colour are formulated by dissolving non-polar dyes in alkanes (typically $\text{C}_{10}\text{--}\text{C}_{16}$). As a large variety of oils and polar liquids can be used, we can adapt our system to the temperature requirements. To contain the oil films on a pixel resolution, we use a thin film fabrication procedure. A black or transparent polymer sheet, typically $50\ \mu\text{m}$ thick, is laser cut to provide the required pixel sizes and patterns. It is then glued onto the insulator-covered substrate with a low viscosity two-part epoxy. Liquids are dosed and the test cells are sealed with an ITO-covered glass slide.

The electro-optic characteristics of a single electrowetting pixel measured at 0° with diffuse illumination are shown in Fig. 2. A small threshold voltage is observed before displacement of the oil film commences. Very little hysteresis in fluid motion is observed. The intermediate optical states are stable, implying that analogue, voltage-controlled grey scales can be realized. At a voltage of about -20 V , the oil film has contracted dramatically and in excess of 70% of the white substrate is exposed, resulting in a reflectivity of about 35% (left-hand axis in Fig. 2). At higher voltages, where the electro-optic curve plateaus, up to 90% of the white substrate becomes exposed. The contraction of the oil results in a maximum contrast of

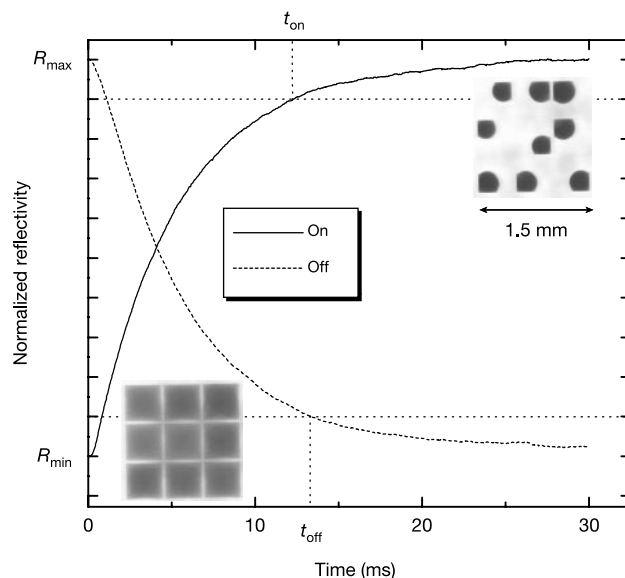


Figure 3 Electrowetting pixel kinetics. Temporal behaviour of a $250 \times 250 \mu\text{m}^2$ pixel, demonstrating the video-speed response. The oil film thickness is $15\ \mu\text{m}$ and the insulator thickness is $0.8\ \mu\text{m}$. The on and off response times are 12 and 13 ms respectively. The reflectivity is shown in normalized units, which does not affect the time axis. t_{on} and t_{off} are defined as the time it takes to complete 90% of the optical modulation. Insets, photographs showing the corresponding optical state for a 3×3 array of $500 \times 500 \mu\text{m}^2$ pixels. With a homogeneous pixel electrode, the observed oil motion is reproducible for a given pixel but is variable between pixels. Motion to a specific position in a pixel array can be realized by using an inhomogeneous pixel electrode (Supplementary Information).

about 15. We determined the contrast (the reflectivity ratio with and without voltage) and the reflectivity at the centre of the absorption band (550 nm), because we used a coloured dye that absorbs only part of the visible spectrum. The full wavelength response (Fig. 2 inset) is indicated for 0 and -20 V . The reflectivity R and contrast obtained are comparable to the optical properties of electrophoretic displays ($R \approx 40\%$ and contrast ~ 11)¹³, and are approaching the optical performance of paper ($R \approx 60\%$ and contrast ~ 15).

The main pixel parameters that influence the electro-optical performance are the thickness of the oil film and the thickness of the fluoropolymer insulator. As the oil film becomes thicker, the electro-optic curve is shifted to higher field strength. As a result, it is best to work with an oil film thickness that is sufficiently thin to give low operating voltage, while sufficiently thick to ensure a satisfactory optical activity (typically around $10\ \mu\text{m}$, that is, nanolitre volumes of oil). The thickness of the insulator determines the necessary field strength as soon as the oil has moved (partly) aside. Hence the insulator should be as thin as possible, while still having sufficient dielectric strength¹⁰.

In small pixels, the motion of the oil film is sufficiently fast to show video content (Supplementary Information). The optically measured response speed in a $250 \times 250 \mu\text{m}^2$ pixel (equivalent to 100 pixels per inch) is shown in Fig. 3. Both the on-switch and the off-switch show a response time close to 10 ms. The on-switch is voltage driven, while the off-switch relies solely on capillary forces to reform the oil film. We have recently commenced the evaluation of larger arrays of electrowetting pixels, and introduced individual pixel addressing (Supplementary Information). Sealed pixel arrays exhibit no deterioration in electro-optic performance after several million switches. The individual pixel addressing in larger-size displays can be provided by active matrix technology.

One of the major drawbacks of current reflective display technologies is their low colour-reflectivity, mostly because of the use of RGB (red-green-blue) colour segmentation¹⁻³. In Fig. 4a we show a

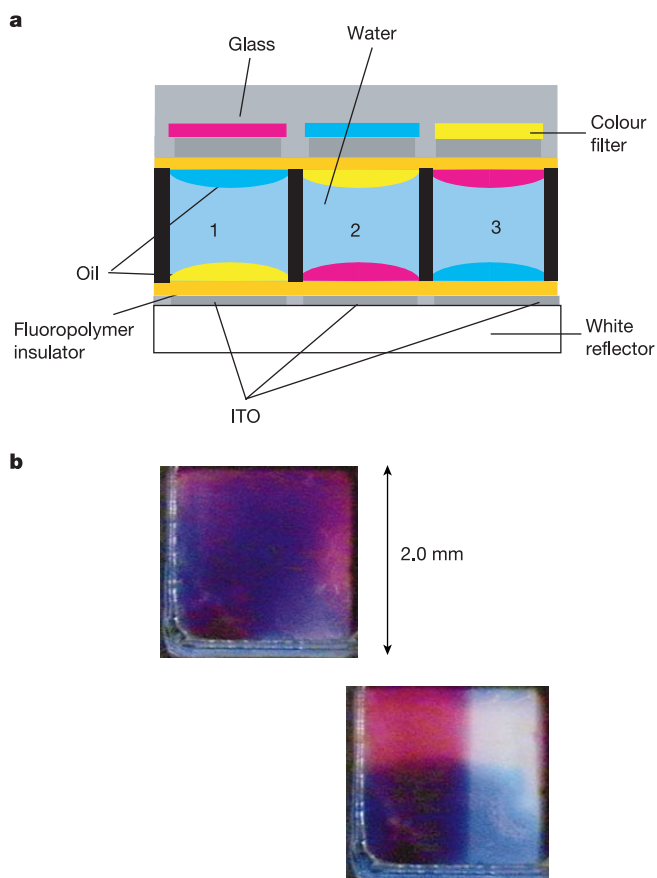


Figure 4 The high-brightness colour electrowetting display principle. **a**, Diagram showing a single subpixelated display pixel with two active layers. **b**, Top view of working cell containing magenta (top) and cyan (bottom) oil films separated by water.

colour concept for an electrowetting display that has a reflectivity that is four times higher than that of a reflective colour liquid-crystal display (LCD) and twice as high as other emerging technologies. In this case, a single display pixel would comprise three subpixels. In each of the subpixels a second oil layer is added, adjacent to the top plate. With a hydrophilic pixel wall, the sandwich structure with two oil layers is the stable equilibrium state. Each oil layer can be switched independently and reversibly by applying a voltage difference between the water and the top or bottom electrode. As for the single layer system, intermediate grey scales can be realized, for each of the two independent switches in a subpixel separately. By using a colour filter, subtractive colour dyes and alternating the colour sequence in the subpixels, we obtain a pixel that has an intrinsic reflectivity that is four times higher than an LCD (67% versus 17%). The oil films can be separated by less than 100 μm , resulting in negligible parallax and a good viewing angle. A demonstration of the independent switching of two layers in a single cell is given in Fig. 4b. Here, the electrodes cover only half of the top and bottom plate, orthogonally oriented with respect to one another. The top layer is magenta and the bottom layer is cyan. As a result, a different optical response is obtained in the bottom left (two layers present), the upper left and bottom right (one layer) and the upper right corner (both layers absent).

We have shown that the microfluidic motion of coloured oil films sandwiched between a solid hydrophobic insulator and water can be precisely and reversibly controlled using a d.c. voltage. We have used this phenomenon to demonstrate electrowetting as a reflective display principle that has very attractive electro-optical characteristics: a reflectivity of over 35%, a contrast of 15 and analogue grey scales. Its high switching speed and a straightforward path to a high-

brightness full colour display set it apart from other emergent electronic-paper technologies. □

Received 16 May; accepted 11 August 2003; doi:10.1038/nature01988.

1. Comiskey, B., Albert, J. D., Yoshizawa, H. & Jacobson, J. An electrophoretic ink for all-printed reflective electronic displays. *Nature* **394**, 253–255 (1998).
2. Sheridan, N. K. *et al.* in *Proc. IDRC97* (ed. Morreale, J.) L82–L85 (Society for Information Display, Toronto, 1997).
3. Podojil, G. M. *et al.* in *SID98 Digest* (ed. Morreale, J.) 51 (Society for Information Display, Anaheim, CA, 1998).
4. Prins, M. W. J., Welters, W. J. J. & Weekamp, J. W. Fluid control in multichannel structures by electrocapillary pressure. *Science* **291**, 277–279 (2001).
5. Grupp, J. in *Eurodisplay Digest 2002* 35–38 (Le Club Visu, SID-France, Nice, 2002).
6. Welters, W. J. J. & Fokkink, L. G. J. Fast electrically switchable capillary effects. *Langmuir* **14**, 1535–1538 (1998).
7. Quilliet, C. & Berge, B. Electrowetting: A recent outbreak. *Curr. Opin. Colloid Interface Sci.* **6**, 34–39 (2001).
8. Berge, B. & Peseux, J. Variable focus lens controlled by an external voltage: An application of electrowetting. *Eur. Phys. J. E* **3**, 159–163 (2000).
9. Pollack, M. G., Fair, R. B. & Shenderov, A. Electrowetting-based actuation of liquid microdroplets for microfluidic applications. *Appl. Phys. Lett.* **77**, 1725–1726 (2000).
10. Seyrat, E. & Hayes, R. A. Amorphous fluoropolymers as insulators for reversible low-voltage electrowetting. *J. Appl. Phys.* **90**, 1383–1386 (2001).
11. Moon, H., Sung, K. C., Garrell, R. L. & Kim, C. J. Low voltage electrowetting-on-dielectric. *J. Appl. Phys.* **92**, 4080–4087 (2002).
12. Beni, G. & Hackwood, S. Electrowetting displays. *Appl. Phys. Lett.* **38**, 207–209 (1981).
13. Ritter, J. in *IDW01 Digest* 343 (Society for Information Display, Nagoya, 2001).

Supplementary Information accompanies the paper on www.nature.com/nature.

Acknowledgements We acknowledge the infrastructural support provided by the Devices, Technology & Services Department, our project colleagues and our team of students (M. Joulaud, J. Guiberteau, R. Massard, E. Morks, A.-S. Dupont, K. Girard, C. Maufrais and P. Jaulneau).

Competing interests statement The authors declare that they have no competing financial interests.

Correspondence and requests for materials should be addressed to R.A.H. (rob.hayes@philips.com) or B.J.F. (johan.feenstra@philips.com).

A combustion-free methodology for synthesizing zeolites and zeolite-like materials

Hyunjoon Lee¹, Stacey I. Zones² & Mark E. Davis¹

¹Chemical Engineering, California Institute of Technology, Pasadena, California 91125, USA

²ChevronTexaco Energy and Research Center, 100 Chevron Way, Richmond, California 94802, USA

Zeolites are mainly used for the adsorption and separation of ions and small molecules, and as heterogeneous catalysts. More recently, these materials are receiving attention in other applications, such as medical diagnosis and as components in electronic devices¹. Modern synthetic methodologies for preparing zeolites and zeolite-like materials typically involve the use of organic molecules that direct the assembly pathway and ultimately fill the pore space^{2–6}. Removal of these enclathrated species normally requires high temperature combustion that destroys this high cost component, and the associated energy release in combination with the formed water can be extremely detrimental to the inorganic structure⁷. Here we report a synthetic methodology that avoids these difficulties by creating organic structure-directing agents (SDAs) that can be disassembled within the zeolite pore space to allow removal of their fragments for possible use again by reassembly. The methodology is shown for the synthesis of zeolite ZSM-5 using a SDA that